Communications, Electronics and Sensing Systems
https://ces-systems.org

X-Ray Topographic Characterization of Crystal Defects in High-Voltage 4H-SiC Wafers

Marie Lehmann

Institute of Photonic Technologies, Faculty of Engineering, Friedrich-Alexander Universität Erlangen-Nürnberg (FAU), Konrad-Zuse-Straße 3/5, 91052 Erlangen, Germany

Editorial correspondence on behalf of the authors: info@ces-systems.org

Abstract

The rapid advancement of high-voltage power electronics has necessitated the development of semiconductor materials capable of withstanding extreme electrical and thermal conditions. Among the various wide bandgap materials, the 4H polytype of silicon carbide has emerged as the premier candidate for next-generation power devices, including those utilized in electric vehicles, renewable energy grid integration, and industrial motor drives. However, the commercial viability and operational reliability of high-voltage silicon carbide devices are fundamentally constrained by the presence of crystallographic defects inherent in the bulk material and epitaxial layers. This paper provides a comprehensive investigation into the characterization of crystal defects in high-voltage 4H-SiC wafers using X-ray topography. We systematically explore the morphological signatures of micropipes, threading screw dislocations, threading edge dislocations, basal plane dislocations, and stacking faults. Through non-destructive X-ray topographic imaging, the spatial distribution and density of these defects are analyzed in detail. The methodology encompasses both laboratory-based and synchrotron white-beam X-ray topography, highlighting the mechanisms of contrast formation based on kinematic and dynamical diffraction theories. Furthermore, the correlation between specific defect types and the degradation of high-voltage device performance is extensively discussed, providing critical insights for material scientists and process engineers aiming to optimize crystal growth and fabrication processes.

Keywords: Silicon Carbide; X-Ray Topography; Crystal Defects; High-Voltage Devices

1. Introduction

1.1 The Role of Silicon Carbide in Power Electronics

The modern landscape of power electronics is undergoing a paradigm shift driven by the urgent global demand for energy efficiency and the electrification of transportation systems. Traditional silicon-based power devices are rapidly approaching their theoretical material limits, particularly in applications requiring high blocking voltages, high switching frequencies, and elevated operating temperatures [1]. In response to these limitations, wide bandgap semiconductors have garnered significant attention from both academic researchers and industrial manufacturers [2]. Among these materials, silicon carbide has established itself as the most mature and commercially viable alternative to silicon for high-power applications [3]. The exceptional physical properties of silicon carbide, including a critical electric field that is approximately ten times higher than that of silicon, a thermal conductivity that rivals that of copper, and a high saturated electron drift velocity, make it uniquely suited for high-voltage power conversion [4].

The 4H polytype of silicon carbide is particularly favored for high-voltage applications due to its superior carrier mobility and isotropic properties compared to other polytypes such as 6H or 3C [5]. Consequently, 4H-SiC wafers serve as the foundational substrate for a wide array of power devices, including Schottky barrier diodes, metal-oxide-semiconductor field-effect transistors, and insulated-gate bipolar transistors [6] [35]. These devices are critical components in the power conversion systems of electric vehicles, solid-state transformers, and high-voltage direct current transmission networks [7]. The deployment of silicon carbide devices in these systems enables significant reductions in system size, weight, and cooling requirements, while simultaneously improving overall energy conversion efficiency [8]. However, the realization of the full potential of high-voltage silicon carbide devices is heavily dependent on the structural quality of the starting wafer material [9].

1.2 The Challenge of Crystallographic Defects

Despite the remarkable progress in silicon carbide bulk crystal growth technology, primarily achieved through the physical vapor transport method, the material remains susceptible to a variety of crystallographic defects [10]. The extreme conditions required for silicon carbide growth, including temperatures exceeding two thousand degrees Celsius and precise control of supersaturation, create a complex thermodynamic environment where defect formation is often unavoidable [11]. These structural imperfections propagate from the bulk substrate into the subsequently grown epitaxial layers, where the active device structures are fabricated [12]. The presence of these defects poses a substantial challenge to the manufacturing yield and long-term reliability of high-voltage devices [13].

Defects in silicon carbide wafers can be broadly categorized into zero-dimensional point defects, one-dimensional line defects, two-dimensional planar defects, and three-dimensional volume defects [14]. While point defects such as vacancies and interstitials influence the electrical properties by acting as recombination centers or traps, it is the extended

crystallographic defects that have the most profound and direct impact on high-voltage device performance [15]. Line defects, including micropipes, threading screw dislocations, threading edge dislocations, and basal plane dislocations, create localized regions of stress and altered electronic structure [16]. Planar defects, such as stacking faults, can severely degrade bipolar device performance through mechanisms such as forward voltage degradation [17]. Understanding the nature, distribution, and density of these defects is therefore of paramount importance for material optimization.

1.3 Objectives and Scope of the Study

To effectively mitigate the detrimental effects of crystallographic defects, it is essential to employ advanced characterization techniques capable of providing detailed, non-destructive, and spatially resolved information across large-area wafers [18]. X-ray topography has proven to be an indispensable tool in this regard, offering unparalleled capabilities for visualizing extended defects in single-crystal materials [19]. The primary objective of this paper is to provide a comprehensive analysis of crystal defects in high-voltage 4H-SiC wafers using X-ray topographic characterization techniques.

This study delves into the fundamental principles of X-ray topography, elucidating how variations in the regular crystal lattice translate into observable contrast on topographic images. We explore both traditional laboratory-based techniques and advanced synchrotron-based methods, highlighting their respective advantages and limitations in resolving complex defect structures [20]. By systematically correlating topographic signatures with specific defect types, this paper aims to establish a clear framework for defect identification and quantification. Furthermore, the implications of these defects on the electrical performance and reliability of high-voltage devices are discussed, providing a crucial link between material science and device engineering [21]. Through this comprehensive examination, the study underscores the critical role of X-ray topography in advancing the state-of-the-art in silicon carbide material quality and device technology.

2. Literature Review and Background

2.1 Evolution of Silicon Carbide Growth Techniques

The historical development of silicon carbide as a semiconductor material is intrinsically tied to the evolution of crystal growth techniques capable of producing large-area, high-quality single crystals. The sublimation method, originally pioneered by Lely in the mid-twentieth century, marked the first successful attempt to grow silicon carbide crystals of sufficient purity for fundamental physical studies [22]. However, the Lely method was characterized by random nucleation, resulting in small, irregularly shaped platelets of various polytypes, which were entirely unsuitable for large-scale device manufacturing. The critical breakthrough occurred with the modification of the sublimation process, known as the seeded sublimation method or physical vapor transport [23].

The physical vapor transport method involves the sublimation of a silicon carbide source powder at high temperatures in an inert gas ambient, followed by the transport of the vapor species along a temperature gradient to condense onto a slightly cooler seed crystal. This technique allowed for the controlled growth of specific polytypes and the progressive scaling of wafer diameters. Over the past few decades, tremendous engineering efforts have been directed towards optimizing the physical vapor transport process [24]. Researchers have meticulously studied the effects of source powder properties, crucible design, thermal field geometry, and ambient gas pressure on the growth kinetics and defect formation. Despite these advancements, the inherent thermal stresses and supersaturation fluctuations during high-temperature growth continue to drive the generation of various crystallographic defects, necessitating rigorous characterization.

2.2 Classification and Characteristics of Crystal Defects

The defect inventory in 4H-SiC is diverse and complex, reflecting the intricate crystal structure and the harsh conditions of its synthesis. Understanding the specific nature of these defects is essential for interpreting X-ray topographic data. Table 1 provides a summary of the primary defect classifications found in 4H-SiC wafers.

Table 1: Defect classifications in 4H-SiC.

Defect Type	Dimensionality	Description and Impact
Micropipes	1D Line Defect	Hollow tubes propagating along the c-axis; causes catastrophic device failure.
Threading Screw Dislocations	1D Line Defect	Dislocations with a Burgers vector parallel to the c-axis; increases leakage current.
Threading Edge Dislocations	1D Line Defect	Dislocations with a Burgers vector perpendicular to the c-axis; impacts oxide reliability.
Basal Plane Dislocations	1D Line Defect	Dislocations lying in the basal plane; primary source of stacking fault expansion.
Stacking Faults	2D Planar Defect	Disruption in the stacking sequence of atomic layers; degrades bipolar operation.

Micropipes were historically the most devastating defects in silicon carbide, consisting of hollow macroscopic tubes that propagate along the c-axis of the crystal [25]. These defects act as open channels through the wafer, leading to immediate and catastrophic breakdown in high-voltage devices. Significant improvements in the physical vapor transport growth process have largely eliminated micropipes in commercial wafers, shifting the focus to solid core dislocations.

Threading screw dislocations are line defects characterized by a Burgers vector that is parallel to the c-axis. They propagate through the crystal roughly parallel to the growth direction. The strain field associated with a threading screw dislocation is substantial, and these defects have been directly linked to localized reductions in the breakdown voltage and localized increases in reverse leakage current in high-voltage devices [26].

Threading edge dislocations, on the other hand, possess a Burgers vector that lies within the basal plane, perpendicular to the c-axis [27]. While their individual strain fields are less intense than those of threading screw dislocations, they are typically present in much higher densities. Threading edge dislocations can form complex networks and low-angle grain boundaries, which can compromise the integrity of gate oxides in metal-oxide-semiconductor devices.

Basal plane dislocations are line defects confined to the basal plane of the crystal lattice. These defects are particularly problematic for high-voltage bipolar devices, such as insulated-gate bipolar transistors and PiN diodes. Under forward bias conditions, the electron-hole recombination energy can facilitate the glide of basal plane dislocations, causing them to dissociate into partial dislocations and form expanding stacking faults [28].

Stacking faults are planar defects that represent an interruption in the normal stacking sequence of the closed-packed bi-layers in the silicon carbide lattice. The formation and expansion of stacking faults introduce localized quantum well states within the wide bandgap, which act as non-radiative recombination centers. This phenomenon, known as bipolar degradation, results in a continuous increase in the forward voltage drop of the device during operation, ultimately leading to device failure [29].

2.3 Impact of Defects on High-Voltage Device Performance

The transition from silicon to silicon carbide in power electronics is primarily motivated by the requirement to operate at higher voltages and temperatures with reduced switching losses. However, the presence of the aforementioned extended defects directly undermines these objectives. The correlation between material defects and device degradation is a central theme in silicon carbide research [30].

When a high reverse bias is applied across a silicon carbide junction, the electric field reaches extreme values. The localized lattice distortion surrounding a threading screw dislocation acts as a region of electric field crowding. This localized field enhancement can initiate premature avalanche breakdown or trap-assisted tunneling, resulting in elevated leakage currents long before the theoretical breakdown voltage of the bulk material is reached. In applications requiring blocking voltages in excess of several kilovolts, the presence of even a single threading screw dislocation within the active area of the device can render it non-functional or unreliable.

Furthermore, the long-term reliability of the silicon dioxide interface on silicon carbide is highly sensitive to the presence of threading edge dislocations. The termination of these dislocations at the semiconductor-insulator interface creates structural irregularities that can trap charge carriers and reduce the time-dependent dielectric breakdown of the oxide layer. This is particularly concerning for trench-gate device architectures, where the electric field is already concentrated at the corners of the trench [31]. Therefore, the comprehensive characterization and mapping of these defects are indispensable steps in the qualification of silicon carbide wafers for high-voltage device fabrication.

3. Methodology of X-Ray Topography Characterization

3.1 Principles of X-Ray Diffraction Topography

X-ray topography is a powerful, non-destructive imaging technique that leverages the principles of X-ray diffraction to visualize the spatial distribution of crystallographic defects within a single crystal. Unlike standard X-ray diffraction techniques that analyze the scattered intensity to determine the average crystal structure, X-ray topography utilizes the diffracted beam to create a two-dimensional spatial map of the diffracting planes. The fundamental physical mechanism governing this process is Bragg diffraction, wherein X-rays of a specific wavelength incident on a crystal lattice are scattered by the parallel atomic planes. Constructive interference occurs only when the path length difference between waves scattered from adjacent planes is an integer multiple of the wavelength, satisfying the specific geometrical conditions defined by the spacing between the planes and the angle of incidence [32].

In a perfectly ordered, ideal crystal, the diffracted X-ray beam maintains a uniform intensity profile across its cross-section. However, when the crystal lattice is disrupted by a defect, such as a dislocation or a stacking fault, the local atomic planes are distorted, bent, or shifted. This localized strain field alters the diffraction conditions in the immediate vicinity of the defect. Depending on the nature of the strain and the specific imaging geometry, the defect region will diffract X-rays with either greater or lesser intensity compared to the surrounding perfect crystal matrix. These variations in diffracted intensity form a contrast image on the detector, effectively mapping the positions and morphologies of the structural imperfections.

The formation of contrast in X-ray topography is generally explained using two theoretical frameworks: kinematic scattering theory and dynamical diffraction theory. Kinematic theory assumes that the incident X-ray beam is weakly scattered and that multiple scattering events can be neglected. In regions of high defect density or strong lattice curvature, the perfect crystal conditions break down, and the volume of material satisfying the Bragg condition increases locally. This results in enhanced diffracted intensity, appearing as a dark contrast region on a photographic positive, a phenomenon known as direct contrast. Dynamical diffraction theory, conversely, accounts for the complex wave interactions and multiple scattering phenomena that occur within thick, nearly perfect crystals. When X-rays propagate through a highly perfect lattice, they undergo an anomalous transmission effect. Defects disrupt this transmission, causing a localized

reduction in intensity, known as dynamical contrast or extinction contrast. In practical topographic imaging of modern silicon carbide wafers, both kinematic and dynamical contrast mechanisms often contribute simultaneously to the final defect image [33].

3.2 Experimental Setup and Parameter Selection

The practical implementation of X-ray topography requires specialized instrumentation and precise alignment. Broadly, the experimental setups can be categorized into laboratory-based systems utilizing characteristic X-ray tubes and large-scale facilities utilizing synchrotron radiation sources. Figure 1 illustrates a typical setup utilized for advanced defect characterization.

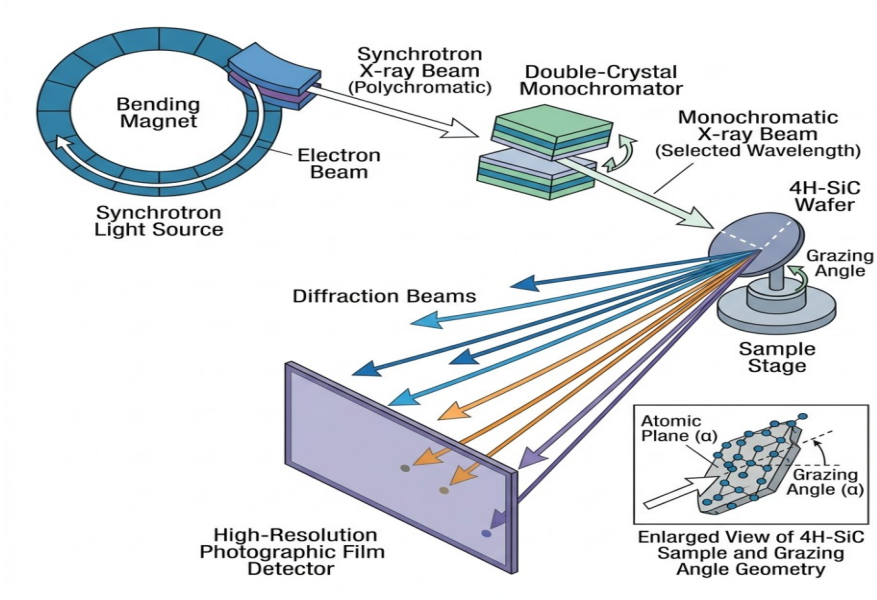

Figure 1: Schematic Overview of the Synchrotron White

Synchrotron white-beam X-ray topography has become the gold standard for characterizing silicon carbide wafers due to the extraordinary brilliance, high flux, and continuous energy spectrum of synchrotron radiation. The continuous spectrum, commonly referred to as white radiation, allows multiple crystal planes to simultaneously satisfy the diffraction conditions, generating a Laue pattern consisting of numerous topographic spots on the detector. Each spot represents a distinct crystallographic reflection, providing a wealth of information from a single exposure. The high intensity of the synchrotron beam enables extremely short exposure times, significantly accelerating the characterization process for large-area wafers.

Table 2 outlines typical experimental parameters considered when conducting X-ray topography on silicon carbide wafers.

Table 2: X-ray topography experimental parameters.

Parameter	Laboratory Setup	Synchrotron Setup
X-Ray Source	Rotating Anode Tube	Storage Ring Bending Magnet
Radiation Spectrum	Monochromatic	Polychromatic White Beam
Penetration Depth	Tens of Micrometers	Entire Wafer Thickness
Resolution	Moderate	Extremely High

The choice of imaging geometry is critical for isolating specific defect types. The two primary modes are transmission geometry and reflection geometry. In transmission geometry, the X-ray beam passes entirely through the bulk of the wafer, and the detector is positioned behind the sample. This mode is excellent for characterizing the bulk defect distribution throughout the entire volume of the substrate, making it ideal for visualizing threading dislocations that propagate along the c-axis. However, for heavily doped silicon carbide wafers, the high absorption of X-rays can necessitate the use of highly energetic, short-wavelength radiation to achieve sufficient transmission.

Reflection geometry, in contrast, involves the incident beam striking the wafer surface at a shallow angle, and the detector capturing the X-rays diffracted back from the surface layers. The penetration depth in this mode is limited to a few micrometers to tens of micrometers, depending on the wavelength and the specific diffraction vector utilized. Reflection topography is particularly valuable for analyzing the quality of thin epitaxial layers grown on the substrate, as it suppresses the background signal from the heavily defective bulk material. By carefully selecting the diffraction vector, researchers can determine the exact direction of the Burgers vector of a dislocation based on the invisibility criterion, which states that a dislocation produces no contrast when its Burgers vector is perpendicular to the diffraction vector.

3.3 Image Processing and Defect Mapping Techniques

The raw data acquired from an X-ray topography experiment, whether recorded on high-resolution nuclear emulsion plates or modern digital detectors, requires careful processing and analysis to extract meaningful quantitative metrics. Historically, topographic analysis relied heavily on the manual inspection of photographic films by experienced

crystallographers, a process that was highly subjective and time-consuming. With the advent of digital imaging and advanced computational algorithms, defect mapping has become increasingly automated and quantitative.

Modern detectors, such as high-resolution charge-coupled device cameras coupled with scintillator screens, allow for direct digitization of the topographic image. The digital images are then subjected to image processing routines designed to enhance contrast, reduce background noise, and isolate distinct defect signatures. Advanced pattern recognition algorithms and machine learning techniques are currently being developed to automatically classify and count different types of dislocations based on their specific shapes and contrast profiles. For instance, threading screw dislocations often appear as large, high-contrast dots with a characteristic lobed structure, while threading edge dislocations manifest as smaller, less intense dots. Basal plane dislocations are typically visualized as curved lines lying within the basal plane.

The ultimate goal of this image processing is to generate comprehensive defect maps that cover the entire area of the silicon carbide wafer. These maps provide spatial coordinates and density distributions for each critical defect category. By superimposing these defect maps with device layout plans, manufacturers can perform spatial correlation studies, predicting the performance and yield of devices before the fabrication process is even complete. This predictive capability is a transformative advantage in the high-cost manufacturing environment of silicon carbide power electronics.

4. Results and Analytical Discussion

4.1 Defect Distribution and Density Analysis

The application of X-ray topography to high-voltage 4H-SiC wafers reveals intricate patterns of defect distribution that are intimately linked to the dynamics of the crystal growth process. Analysis of full-wafer topographs typically indicates that defect densities are not uniform across the wafer area. Instead, strong radial and azimuthal variations are frequently observed, reflecting the thermal gradients and stress distributions present during physical vapor transport growth.

Table 3 presents a representative analysis of defect density measurements taken from different regions of a commercial 4H-SiC wafer.

Table 3: Defect density measurements across different wafer regions.

Defect Type	Center Region Density	Mid-Radius Region Density	Edge Region Density
Threading Screw	Low	Moderate	High
Threading Edge	Moderate	High	Very High
Basal Plane	Low	Low	Moderate
Stacking Faults	Very Low	Low	Moderate

The central region of the wafer, corresponding to the initial nucleation site on the seed crystal, often exhibits a relatively low density of threading screw and basal plane dislocations. The thermal conditions in this central zone are typically more stable and symmetric, promoting high-quality crystal growth. However, as the growth front expands radially outwards, the thermal gradients become steeper, and the thermoelastic stresses within the growing boule increase substantially. This stress concentration is the primary driving force for the multiplication and glide of dislocations.

Consequently, the mid-radius and edge regions of the wafer consistently display significantly higher defect densities. Threading edge dislocations, in particular, tend to arrange themselves into cellular network structures or low-angle grain boundaries at the wafer periphery to minimize the total strain energy of the crystal. These low-angle grain boundaries appear as continuous lines of dark contrast in transmission topographs, separating regions of the crystal with slight misorientations. The presence of these boundaries indicates a significant degradation of the single-crystal quality and poses a severe risk to large-area power devices fabricated in these outer regions.

Furthermore, the mapping of basal plane dislocations provides critical feedback for the optimization of epitaxial growth processes. Through carefully controlled epitaxial growth techniques, it is possible to convert a large fraction of substrate basal plane dislocations into threading edge dislocations at the substrate-epitaxial interface. X-ray topography in reflection mode is routinely used to verify the efficiency of this conversion process by comparing the basal plane dislocation density in the substrate with that in the active epitaxial layer.

4.2 Correlation with Wafer Processing and Device Yield

The quantitative defect data extracted from X-ray topographic characterization serves as a fundamental metric for evaluating the efficacy of wafer processing techniques and predicting the ultimate yield of high-voltage devices. The relationship between specific topographic defect signatures and device failure modes is a critical area of ongoing investigation. By combining X-ray topography with electrical testing methodologies such as deep level transient spectroscopy and current-voltage profiling, researchers can establish direct correlations between structural imperfections and electrical degradation.

Table 4 summarizes the established correlations between primary defect types and the dominant failure modes observed in high-voltage silicon carbide devices.

Table 4: Correlation between defect types and high-voltage device failure modes.

Defect Type	Primary Device Impact	Dominant Failure Mode
Threading Screw	Enhanced Localized Electric Field	Premature Avalanche Breakdown
Threading Edge	Interface State Generation	Gate Oxide Reliability Degradation
Basal Plane	Nucleation of Planar Defects	Forward Voltage Drift
Stacking Faults	Non-Radiative Recombination	Bipolar Current Gain Reduction

The correlation analysis consistently demonstrates that the elimination of threading screw dislocations is paramount for achieving the theoretical blocking voltage capability of 4H-SiC. Devices fabricated over regions containing high densities of threading screw dislocations inevitably exhibit excessive reverse leakage currents and fail at voltages significantly below the design threshold. This spatial correlation allows manufacturers to strategically locate critical device structures away from heavily defective regions, thereby maximizing the usable area of the wafer and improving overall yield.

Moreover, the detection and mapping of basal plane dislocations and their subsequent expansion into stacking faults during device operation is a vital application of X-ray topography. Topographic imaging before and after electrical stress testing provides unambiguous evidence of stacking fault expansion driven by electron-hole recombination. This phenomenon is a primary roadblock to the commercialization of ultra-high-voltage bipolar devices, such as those rated for ten kilovolts and above. The detailed characterization of these planar defects using topography guides the development of specialized buffer layers and defect-mitigation structures designed to suppress the formation and expansion of stacking faults, thereby ensuring the long-term operational stability of advanced power infrastructure components [34].

5. Conclusion

5.1 Summary of Characterization Findings

The comprehensive characterization of high-voltage 4H-SiC wafers is an essential prerequisite for the advancement of next-generation power electronics. This study has detailed the critical role of X-ray topography as a sophisticated, non-destructive analytical technique capable of resolving the complex defect structures inherent in silicon carbide crystals. By thoroughly investigating the principles of diffraction and contrast formation, we have elucidated how extended defects, such as threading screw dislocations, threading edge dislocations, basal plane dislocations, and stacking faults, can be precisely identified and mapped across large-area substrates. The utilization of both laboratory and synchrotron-based topographic methods provides a versatile toolkit for interrogating the crystalline quality from the bulk volume to the thin epitaxial layers where active device operation occurs.

The analytical results demonstrate that defect distribution in commercial wafers is highly inhomogeneous, heavily influenced by the thermal and mechanical stresses experienced during the high-temperature physical vapor transport growth process. The concentration of extended defects and low-angle grain boundaries at the wafer periphery remains a significant hurdle for maximizing the yield of large-area, high-current devices. Crucially, the direct correlation established between specific topographic defect signatures and electrical failure modes underscores the indispensability of spatial defect mapping in modern manufacturing environments.

5.2 Future Outlook and Advancements

As the demand for silicon carbide power devices continues to surge, driven by the electrification of the automotive sector and the modernization of energy grids, the requirements for material perfection will become increasingly stringent. Future advancements in X-ray topographic characterization must focus on enhancing the speed, resolution, and automated analytical capabilities of the technique. The development of high-brilliance, compact laboratory X-ray sources could democratize access to high-resolution topography, reducing the reliance on scarce synchrotron beamtime for routine quality control. Furthermore, the integration of advanced artificial intelligence and machine learning algorithms for the automated recognition, classification, and quantification of defect contrast patterns will significantly accelerate the feedback loop between material characterization and crystal growth optimization. By continuing to refine these characterization methodologies, the scientific community can pave the way for the realization of defect-free, ultra-high-voltage silicon carbide devices, solidifying their foundational role in the sustainable energy landscape of the future.

References

1. Chen, B. L., Zhang, J. Y., Xu, W. J., Yan, S. Y., & Zhu, X. Q. (2025). Thermodynamic and kinetic studies of mononuclear non-heme high-valent (FeO) 2+ complexes. ACS omega, 10 (4), 3718.
2. Luan, S., Wang, P., Zhang, L., He, Y., Huang, X., Jian, G.,... & Fu, Z. (2023). Atmospherically hydrothermal assisted solid-state reaction synthesis of ultrafine BaTiO3 powder with high tetragonality. Journal of Electroceramics, 50 (4), 97-111.
3. Li, H., Zheng, T., Peng, Y., & BouDagher-Fadel, M. K. (2023). The fusulinids in a middle-late Permian carbonate platform (from Maokou to Wuchiapingian stage) in eastern Sichuan Basin, China. In Stratigraphy & Timescales (Vol. 8, pp. 413-435). Academic Press.
4. Pabon, J. J. G., Wang, J., Chamanehpour, E., Salami, D., & Khosravi, A. (2025). Dynamic integration of solar-powered hydrogen systems with fuel cells and district heating for green data centers. International Journal of Hydrogen Energy, 196, 152557.
5. Zhang, K. X., Chen, Z. Y., Hu, S. S., Zhang, J. P., Li, Y. Z., Wu, D. L., ... & Soukhojak, A. (2026, August). Observation and Analysis of the “Galaxy” Defect in 4H-SiC through X-Ray Synchrotron Topography. In Defect and Diffusion Forum (Vol. 452, pp. 73-78). Trans Tech Publications Ltd.
6. Luan, S., Si, S., Zhang, L., Wang, P., Jian, G., Yang, J.,... & Cao, X. (2023). Fabrication of BaTiO3 nanopowders with high tetragonality via two-step assisted rotary furnace calcination for MLCC applications. Ceramics International, 49 (8), 12529-12539.
7. Yang, Y., Hu, H., Li, W., Li, S., Yang, J., Zhao, Q., & Zhang, C. (2023, June). Flow to control: Offline reinforcement learning with lossless primitive discovery. In Proceedings of the AAAI Conference on Artificial Intelligence (Vol. 37, No. 9, pp. 10843-10851).
8. Yang, Y., Ma, X., Li, C., Zheng, Z., Zhang, Q., Huang, G., ... & Zhao, Q. (2021). Believe what you see: Implicit constraint approach for offline multi-agent reinforcement learning. Advances in Neural Information Processing Systems, 34, 10299-10312.
9. Lv, X., Liu, S., Wang, P., Mohammad-Rezaei Bidgoli, E., & Arefi, M. (2023). On the dynamics and wave propagation of reinforced composite nanosystem. Engineering with Computers, 39(1), 151-171.
10. Wang, Y., Lou, M., Liang, W., & Zhang, C. (2023). Numerical and experimental investigation on tensile fatigue performance of reinforced thermoplastic pipes. Ocean Engineering, 287, 115814.
11. Chen, Z. Y., Zhang, J. P., Hu, S. S., Zhang, K. X., Li, Y. Z., Wang, H. C., ... & Dudley, M. (2026, June). Investigation of Spoke Pattern of Stacking Faults in 4H-SiC Wafers Grown by Physical Vapor Transport Method. In Materials Science Forum (Vol. 1190, pp. 55-62). Trans Tech Publications Ltd.

12. Chen, B. L., Jing, S., & Zhu, X. Q. (2023). Thermodynamics Evaluation of Selective Hydride Reduction for α, β-Unsaturated Carbonyl Compounds. Molecules, 28 (6), 2862.
13. Hu S, Chen Z, Zhang K, et al. Stacking fault analysis for the early-stages of PVT growth of 4H-SiC crystals[J]. Journal of Crystal Growth, 2026, 681: 128523.
14. Chen, B. L., Yan, S. Y., & Zhu, X. Q. (2023). A Mechanism study of redox reactions of the ruthenium-oxo-polypyridyl complex.Molecules,28(11), 4401.
15. Ma, Y., & Qu, D. (2026). Machine Learning Based Markov Decision Framework for Optimizing Circular Economy Systems.Engineering Proceedings,120(1), 44.
16. Wang, X., Wang, P., Jiang, W., Wu, F., Kiani, M., & Arefi, M. (2021). Mathematical and computer simulation for Electro-Magneto-Thermo-Elastic Buckling of the Porous Nano system. Structural Engineering and Mechanics, 80(2), 231-242.
17. Wang, Y. Y., Lou, M., Wang, Y., Wu, W. G., & Yang, F. (2022). Stochastic failure analysis of reinforced thermoplastic pipes under axial loading and internal pressure. China Ocean Engineering, 36(4), 614-628.
18. Luan, S., Tang, M., Mu, H., Yu, J., Wang, P., & Zhang, L. (2025). A co-precipitation route to produce BaTiO3 nanopowders with high tetragonality for ultra-thin MLCCs application. Journal of Materials Science: Materials in Electronics, 36 (9), 526.
19. Liu, J., & Huang, Y. (2026). GBMP-LCA: A Gradient Boosting–Based Framework for Performance Prediction and Life-Cycle Optimization of Green Building Materials. Fundamental Scientific Reports in Multidisciplinary Areas, 2 (02), 193-204.
20. Lu, W., & Wang, J. (2025). Accumulated Performance Comparison of Solar PV and Solar Thermal Water Heating in New Zealand. Engineering Reports, 7(12), e70526.
21. Peng, Y., Li, H., BouDagher-Fadel, M., Wang, L., Zhang, D., Zheng, T., & Yang, K. (2022). Benthic foraminifera distribution and sedimentary environmental evolution of a carbonate platform: A case study of the Guadalupian (middle Permian) in eastern Sichuan Basin. Marine Micropaleontology, 170, 102079.
22. Zhu, Q., & Chen, H. (2025, August). Bias correction of wind forecasts from the noaa global ensemble forecast system (gefs) using machine learning. In IGARSS 2025-2025 IEEE International Geoscience and Remote Sensing Symposium (pp. 4637-4640). IEEE.
23. Wang, J. (2026). A comparative conceptual analysis of CO2 heat pump dryers with closed-loop and open-loop air cycles. Energy Conversion and Management, 352, 121093.
24. Zhou, X., Wang, P., Al-Dhaifallah, M., Rawa, M., & Khadimallah, M. A. (2022). A machine learning-based model for the estimation of the critical thermo-electrical responses of the sandwich structure with magneto-electro-elastic face sheet. Advances in nano research, 12(1), 81-99.
25. Yang, Z., Hu, D., Guo, Q., Zuo, L., & Ji, W. (2023). Visual E 2 C: AI-driven visual end-edge-cloud architecture for 6G in low-carbon smart cities. IEEE Wireless Communications, 30(3), 204-210.
26. Wan, H., Cheng, J., Deng, Y., Wu, D., Chen, Y., Lin, Z., ... & Ji, X. Towards Physics Aware Embodied Control with Graph based Object-centric Learning. ACM Transactions on Cyber-Physical Systems.
27. Chen, B., Hu, X., & Zhu, X. (2023). Essential Rule Derived from Thermodynamics and Kinetics Studies of Benzopyran Compounds.Molecules,28(24), 8039.
28. W. Zhang, "A 5-6 GHz PVT Robust Current Mode Passive Mixer for Direct Down-Conversion Receiver," in *2026 5th International Conference on Electronics, Integrated Circuits and Communication Technology (EICCT)*, 2026, pp. 420–424.
29. Li, X., Wang, P., Li, G., & Zhang, Y. (2023). Design of a novel self-test-on-chip interface ASIC for capacitive accelerometers. IEEE Transactions on Circuits and Systems I: Regular Papers, 70(7), 2834-2843.
30. Yao, Jingyu, et al. "Explainable AI Enhanced Traffic Forecasting for Proactive Autonomous Vehicle Routing." 2026 IEEE Conference on Technologies for Sustainability (SusTech). IEEE, 2026.
31. Li, Y. Z., Zhang, J. P., Chen, Z. Y., Wang, H. C., Zhang, K. X., Hu, S. S., ... & Dudley, M. (2026, August). Growth and Characterization of High-Quality Thick Epitaxial 4H-SiC Wafers for High Voltage Devices. In Defect and Diffusion Forum (Vol. 452, pp. 79-85). Trans Tech Publications Ltd.
32. Lu, J., Fang, Y., Yang, X., Hu, W., Tuo, J., & Zhang, F. (2025). Modal Metamodeling-Based Uncertainty Propagation for Frequency Response in Non-Proportional Damping Systems. International Journal of Structural Stability and Dynamics, 2650279.
33. Yang, Y., Wang, Q., Li, C., Hu, H., Wu, C., Jiang, Y., ... & Xu, B. (2025, May). Fewer may be better: Enhancing offline reinforcement learning with reduced dataset. In International Conference on Learning Representations (Vol. 2025, pp. 7076-7098).
34. Xiong, S., Chen, T., Rupendra, A., Clement, C., Gasparri, E., & Lucchi, E. (2026). Embodied Carbon of Progressive Timber Integration in a 47-Storey Tropical High-Rise: A Singapore Public Housing Case Study. Building and Environment, 114910.
35. Li, Y., Zhou, Y., Zhang, Y., Wang, P., Zhang, Y., Li, X., & Zhang, X. (2025). Nonvolatile Optical Switch With a Programmable pn Heterojunction.IEEE Transactions on Electron Devices,72(8), 4030-4035.